

Tailored Nanostructuring of End-Group-Functionalized High-Density Polyethylene Synthesized by an Efficient Catalytic Version of Ziegler's "Aufbaureaktion"**

Saravana K. T. Pillai,^[a] Winfried P. Kretschmer,^[a] Martin Trebbin,^[b]
Stephan Förster,^[b] and Rhett Kempe^{*[a]}

Polyethylene (PE) is the most widely used synthetic polymer and is essential for our modern life style due to its low cost and its broad applicability. Unfortunately, the compatibility with other important polymers or materials is limited. Compatibility agents with a PE block and a block of that other polymer or a block that is compatible with the material could solve this problem. Furthermore, PE-based block copolymers may allow to nanostructure PE through microphase separation and enable new applications of this commodity. Both approaches rely on an efficient synthesis of PE having an end group that allows the easy introduction of the second polymer block. A polymerization method that produces metal-terminated PE which can easily be converted into PE carrying such reactive end groups is coordinative chain-transfer polymerization (CCTP).^[1,2] Pioneering work was done by Eisenberg and Samsel,^[3] as well as Mortreux and co-workers.^[4] Meanwhile, a few ethylene/propylene CCTP catalyst systems by using rare-earth metals (REM) and transition metals in combination with different chain-transfer agents (CTA), such as Mg, Zn,^[5,6,7] and Al alkyls,^[8,9] have been disclosed. Furthermore, enhancements of the CCTP concept, such as "chain shuttling" and "ternary CCTP", have been developed.^[10] Mechanistic studies have been carried out by the Bochman's^[11] and the Norton's group.^[12,13] The kinetic of chain growth catalyzed by $[(\text{EBI})\text{Zr}(\mu\text{-Me})_2\text{AlMe}_2][\text{B}(\text{C}_6\text{F}_5)_4]$ (EBI = ethylene-bridged bis(indenyl)) has been studied. The reaction is first order in [olefin] and [catalyst] and inverse first order in $[\text{AlR}_3]$.^[12]

These inverse first-order dependencies prohibit the use of high CTA/catalyst ratios. High amount of CTA resulted in an overall poor polymerization activity. As a consequence, most of the described CCTP catalyst systems worked with CTA/catalyst ratio smaller than 500 and became inactive with significantly higher CTA/catalyst ratio. This problem could be solved by the design of new catalyst systems that undergo fast chain growth compared to chain exchange and still suppress β -H elimination/transfer processes. In such a regime, multiple insertions may compensate efficiency loss caused by high CTA/catalyst ratio.^[14]

Herein, we report a new titanium-based catalyst system that is highly active in the presence of very high CTA/catalyst ratio and undergoes polyethylenyl chain transfer to triethylaluminum (TEA). No β -hydride elimination/transfer products were observed. This polymerization process can be viewed as an efficient catalytic version of Ziegler's "Aufbaureaktion". Through oxidation with O_2 and subsequent hydrolytic work-up, the metallopolymers can be converted to PE-OH in high yield. The generated PE-OH was used to synthesize block copolymers with polylactide (PLA) as a counterblock. Microphase separation gave different morphologies by varying the PLA block length. Etching out of the sacrificial PLA block gave rise to mesoporous polyethylene and polyethylene nanofibers/ribbons.

Nanoporous PE has been generated from hydrogenated 1,4-polybutadiene (hPB). Block copolymers from hPB and polystyrene obtained by anionic polymerization allow excellent structuring, but need rather harsh and difficult conditions to control etching processes to remove the polystyrene block.^[15] Furthermore, polymeric bicontinuous microemulsion templates were generated by using hPB and block copolymers carrying a hPB block.^[16] Unfortunately, the PE mimic hPB suffers from the unavoidable presence of branches. Ring-opening metathesis polymerization of cyclooctene was discussed as an alternative and gave rise to pseudo PE blocks after hydrogenation. Triblock copolymers carrying this block were successfully converted into porous PE.^[17] The fabrication of polyethylene nanofibers/ribbons through the block copolymer approach has not been reported yet.^[18,19] End-group-functionalized PE synthesized by CCTP was already used to make block copolymers,^[5d,e,9c,20] among them PE-PLA block copolymers.^[5e]

[a] S. K. T. Pillai, Dr. W. P. Kretschmer, Prof. Dr. R. Kempe
Lehrstuhl Anorganische Chemie II
Universität Bayreuth
Universitätsstrasse 30, NW I
95440 Bayreuth (Germany)
Fax: (+49) 921552157
E-mail: kempe@uni-bayreuth.de

[b] M. Trebbin, Prof. Dr. S. Förster
Lehrstuhl Physikalische Chemie I
Universität Bayreuth
Universitätsstrasse 30, NW I
95440 Bayreuth (Germany)

[**] Aufbaureaction (German): buildup reaction.

Supporting information for this article is available on the WWW under <http://dx.doi.org/10.1002/chem.201202506>.

Recently, we developed REM-based CCTP catalysts^[8,21] and varied the nature as well as the steric bulk of the mono-anionic ligand used. In addition, the size of the REM atom was varied to find a catalyst system that tolerates high CTA/catalyst ratio.^[9f,g,22] Unfortunately, these variations did not lead to CTA/catalyst ratio above 500. Thus, our attention was shifted to Group 4 metals, especially, towards titanium catalysts. Titanium catalysts stabilized by bulky aminopyridinato (Ap) ligands showed attractive polymerization activities, however, suffered from ligand-transfer problems.^[23]

The Ap ligand was transferred to the CTA (aluminum alkyls) and a higher electron-donor ability of the ligand increased ligand-transfer rates instead of decreasing them.^[24] Bulky guanidines^[25] are chemically related to Ap ligands and were expected to change the ligand-transfer rates, but may instead maintain high polymerization activity.

The reaction of amido titanium trichloride complexes^[26] with *N,N'*-methanediylidenebis(2,6-diisopropylaniline) led to the complexes **A**, **B**, and **C** through methanediimine insertion into the titanium–amide bonds (Figure 1). NMR spectra showed a single signal set for the symmetrically substituted complexes **A** and **C**. Signal splitting was observed for complex **B** indicating a dynamic behavior, presumably rotation around the C–N bond of the noncoordinated nitrogen atom. Variable temperature NMR studies indicated a coalescence temperature of 88°C for the methine proton signal of the isopropyl groups and a rotation barrier of about 73 kJ mol⁻¹. X-ray diffraction crystal-structure analysis of **A** and **B** revealed monoguanidinate trichloro complexes and a distorted trigonal bipyramidal coordination of the titanium atoms. The variation of the substituents at the noncoordinated nitrogen atom only slightly altered the titanium coordination (Figure 1, bottom).

Ethylene polymerization studies by using complex **A** as a precatalyst and different activation protocols revealed that

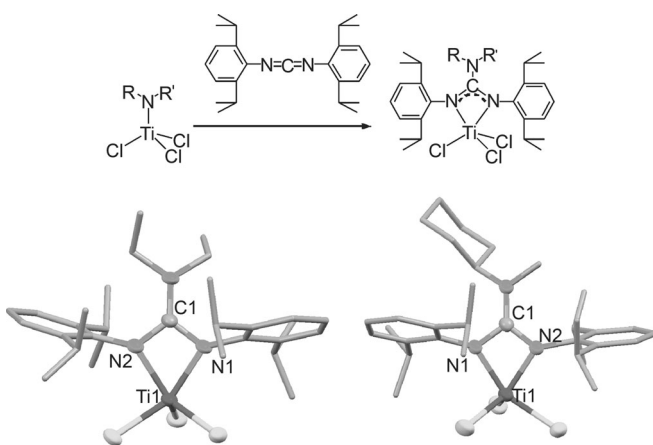


Figure 1. Polymerization precatalyst synthesis and structure. Top: synthesis of the complexes **A** ($R=R'=\text{ethyl}$), **B** ($R=\text{cyclohexyl}$, $R'=\text{methyl}$), and **C** ($R+R'=\text{pentamethylene}$). Bottom: molecular structure of **A** and **B** determined by X-ray diffraction single-crystal structure analysis. Selected bond lengths [Å] and angles [°] of **A** (bottom left): N1–Ti1 2.015(3), N2–Ti1 2.027(4), N1–C1–N2 106.0(3); and of **B** (bottom right): Ti1–N1 2.0081(14), Ti1–N2 2.0180(15), N1–C1–N2 106.40(14).

A can be highly active, if activated with MAO (methyl alumoxanes), d-MAO (dry MAO, free trimethyl aluminum content of MAO was removed), and a combination of aluminum alkyls and perfluoroarylborates (Table 1).^[27] Investi-

Table 1. Initial polymerization studies by using complex **A**. Conditions: **A** (2 µmol), ethylene pressure (2 bar), toluene (150 mL), polymerization time (15 min), ammonium borate: $[R_2N(CH_3)_2H]^+[B(C_6F_5)_4]^-$ ($R=C_{16}H_{33}-C_{18}H_{37}$), Ti/B = 1:1.1 (TMA = trimethyl aluminum, TiBA = tri-isobutyl aluminum).

Run	Activator	T [°C]	M _{pol.} [g]	Activity [kg _{PE} mol ⁻¹ h ⁻¹ bar ⁻¹]	M _n [g mol ⁻¹]	M _w / M _n
1	d-MAO ^[a]	30	3.64	3640	141000	5.9
2	d-MAO ^[a]	50	1.36	1360	52000	3.2
3	d-MAO ^[a]	80	1.22	1220	28000	2.7
4	MAO ^[b]	30	2.82	2820	16000	2.0
5	MAO ^[b]	50	1.67	1670	8400	2.5
6	MAO ^[b]	80	0.1	100	7700	4.0
7	TMA/B- (C ₆ F ₅) ₄ ^[c]	50	0.7	700	3900	1.9
8	TEA/B- (C ₆ F ₅) ₄ ^[c]	50	1.62	1620	2200	1.9
9	TIBA/B- (C ₆ F ₅) ₄ ^[c]	50	1.1	1100	40000	2.0
10	TEA/B- (C ₆ F ₅) ₄ ^[d]	50	1.8	1800	1800	1.9
11	TEA/B- (C ₆ F ₅) ₄ ^[d,e]	50	3.7	930	2300	1.7
12	TEA/B- (C ₆ F ₅) ₄ ^[d,f]	50	7.0	880	2300	1.7

[a] Ti/Al = 1:650; [b] Ti/Al = 1:500; [c] Ti/Al = 1:500; [d] Ti/Al = 1:1000; [e] 60 min; [f] 120 min.

gations at different temperatures revealed that the catalyst is stable in the temperature window between 30 and 80°C. Activation by MAO and d-MAO led to significant differences of the molecular weight of the polymers indicating a polymethyl chain-transfer catalysis to aluminum (Table 1, run 1–6). ¹H NMR spectroscopy investigations of the hydrolyzed polymers obtained by MAO activation support this hypothesis, because no olefinic end groups were detected. Polymerization reactions by using a borate activator and different aluminum alkyls (Table 1, run 7–9) indicated that TEA is a better transfer agent than trimethylaluminum (TMA). A CCTP mechanism with a very fast chain transfer compared with chain growing did not seem to operate. The molecular weight of the polymers did not increase with increased polymerization time (Table 1, run 10–12). In a time regime from 15 to (60 to) 120 min a larger amount of polymer with essentially the same molecular weight was produced. The number of aluminum alkyl chains extended increases from 17 to (27 to) 50%, respectively. Control over the molecular weight can be obtained by the catalyst, the temperature, and the CTA to catalyst ratio (Table 2). The molecular weight of the polymers decreased with CTA/catalyst ratio increasing from 500 to 1000 (Table 2). Furthermore, different catalysts have different insertion rates leading to different molecular weights of the polymers at the same CTA/catalyst ratio (Table 2). Polymerization run at very high CTA/catalyst

Table 2. Ethylene polymerization studies by using complexes **B** and **C**, activation with TEA and ammonium borate. Conditions: precatalyst (2.0 μmol), ammonium borate (2.2 μmol ; $[\text{R}_2\text{N}(\text{CH}_3)\text{H}]^+[\text{B}(\text{C}_6\text{F}_5)_4]^-$ ($\text{R} = \text{C}_{16}\text{H}_{33}-\text{C}_{18}\text{H}_{37}$)); Ti/B = 1:1.1; CTA = TEA; toluene (150 mL); $T = 50^\circ\text{C}$; $p = 2$ bar; $t = 15$ min.

Run	Precat.	Al/Ti	$M_{\text{pol.}}$	Activity	M_n	M_w/M_n
		[g]		[$\text{kg}_{\text{PE}} \text{mol}_{\text{cat}}^{-1} \text{h}^{-1} \text{bar}^{-1}$]	[g mol^{-1}]	
1	B	500	1.70	1700	2800	2.2
2	B	750	1.75	1750	2100	2.0
3	B	1000	1.80	1800	1600	2.0
4	C	500	1.40	1400	3100	2.4
5	C	750	1.40	1400	2700	2.4
6	C	1000	1.55	1550	2500	2.3

ratio were performed and subsequently oxidized by using O_2 as an oxidant to give PE-OH (Table 3). Aluminum alkyl chains (78%) of run 1 in Table 3 were extended. Remark-

Table 3. Ethylene polymerization studies by using complex **A**, activation with TEA and ammonium borate, and subsequent oxidation by O_2 . Conditions: ammonium borate $[\text{R}_2\text{N}(\text{CH}_3)\text{H}]^+[\text{B}(\text{C}_6\text{F}_5)_4]^-$ ($\text{R} = \text{C}_{16}\text{H}_{33}-\text{C}_{18}\text{H}_{37}$); Ti/B = 1:1.1; CTA = TEA; toluene (150 mL); $p = 5$ bar; $t = 60$ min.

Run	A [μmol]	Al/Ti	T [$^\circ\text{C}$]	$M_{\text{pol.}}$ [g]	Activity [$\text{kg}_{\text{PE}} \text{mol}_{\text{cat}}^{-1} \text{h}^{-1} \text{bar}^{-1}$]	M_n [g mol^{-1}]	M_w/M_n
1	4 ^[a]	2500	50	44.0	5500	1700	1.8
2	2	5000	70	47.0	4700	2100	1.9
3	0.6	17000	65	28.4	9470	2500	1.8
4	0.4	25000	60	32.0	16000	3300	1.9
5	0.3	33000	65	24.4	16300	2500	1.9
6	0.2	50000	60	16.7	16700	2900	1.9

[a] $p = 2$ bar.

bly, the catalyst based on **A** showed activities of around 16000 $\text{kg}_{\text{PE}} \text{mol}_{\text{cat}}^{-1} \text{h}^{-1} \text{bar}^{-1}$ in the presence of 25000, 33000, or 50000 equivalents of TEA. The catalyst performance decreased slightly during the last 45 min of the one hour polymerization experiments indicating a good stability of the catalyst system at 60 to 70°C. Oxidation of the aluminum-terminated PE led to PE-OH (after hydrolytic work-up).

The PE-OH produced in run 4 in Table 3 was used for diblock copolymer synthesis. As was determined by NMR spectroscopy, it contained 80% of hydroxyl-group-functionalized PE. PLA was chosen as sacrificial counterblock, because diblock-copolymer formation based on OH end groups was established, and PLA can adopt an amorphous form, which is in good contrast to the crystalline nature of linear PE.^[5e,28] Moreover, PLA can be etched out under mild basic conditions without disrupting the PE structure of the microphase-separated diblock copolymer.^[17] Tin(II) 2-ethylhexanoate $[\text{Sn}(\text{Oct})_2]$ was used as a catalyst to polymerize a PLA block onto PE-OH. Different amounts of *rac*-lactide gave rise to PE-PLA diblock copolymers with different PLA block lengths [PE-PLA(1) and (2)]. The diblock copolymers were characterized by high-temperature gel-permeation chromatography (GPC), NMR, TGA, differential scanning calorimetry (DSC), and IR analyses. Different

nanostructuring of PE-PLA(1) and (2) through microphase separation were accomplished in cumene (Figure 2). The diblock copolymers were dissolved in cumene at 152°C followed by slow solvent casting in oil bath at 140°C. The melt was subsequently annealed at this temperature for six hours. Annealing of the melt seemed to ensure good segregation of the equilibrated nanostructures (Table 4).

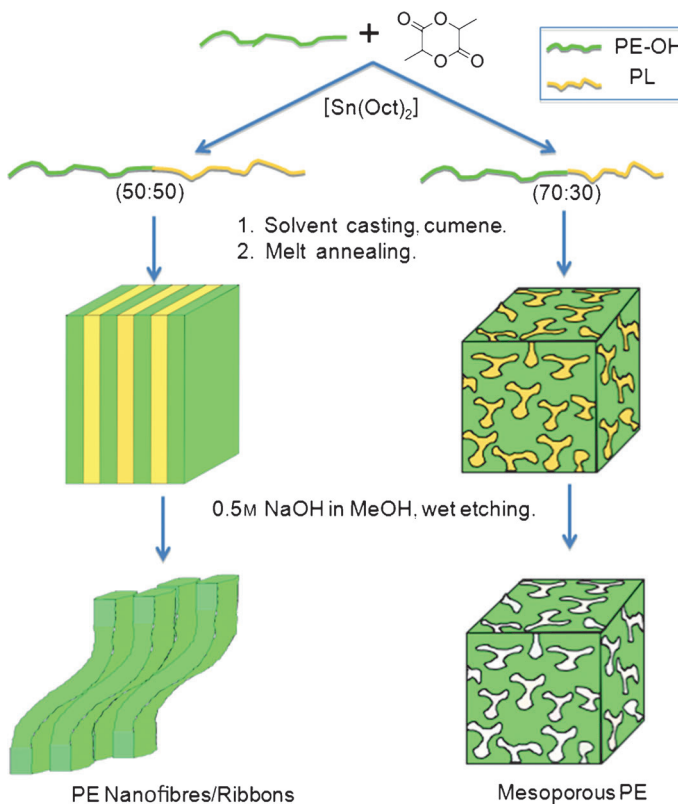


Figure 2. Schematic representation of the synthesis of mesoporous polyethylene and polyethylene nanofibers/ribbons.

The microphase-separated diblock copolymers were investigated by synchrotron small-angle X-ray scattering (SAXS; Figure 3) and atomic-force microscopy (AFM). AFM data, recorded at ambient condition in nondestructive tapping mode, indicated a rather well-ordered lamellar type of structuring for PE-PLA(1) and a less ordered bicontinuous morphology for PE-PLA(2) (Figure 4a and b and Figure 5a, respectively).

Synchrotron SAXS studies are in agreement with these observations (Figure 3). The SAXS pattern of PE-PLA(1) with three peaks at $q = 0.29$, 0.58 , and 0.85 nm^{-1} correspond to the ratio of 1:2:3 indicating a lamellar structure (Figure 3). Calculations performed by using the software “Scatter” confirmed this alternating lamellar lattice with periodic domain spacing (d spacing) of 20 nm.^[32] Furthermore, the first-order peak at 0.28 nm^{-1} was used to confirm the d spacing. Observation of such large domain spacing for these lower molecular weight copolymers might be caused by the polydispersity of PE block and the presence of 20% of the homopolymer in the sample.^[33] The SAXS pattern of PE-

Table 4. Summary of the characterization data of the diblock copolymers.

Sample ID	PE-OH	PE-PLA(1)	PE-PLA(2)
$M_n^{[a]}$ [g mol ⁻¹]	3300	4500	4000
PDI ^[a]	1.9	1.7	1.6
$M_w^{[b]}$ [g mol ⁻¹]		5500	4400
$f_{\text{PLA}}^{[c]}$		0.44	0.38
$T_m^{[d]}$ [°C]	130.0	126.6	127.2
$T_c^{[d]}$ [°C]	115.0	113.1	114.0
$\Delta H_m^{[d]}$ [J g ⁻¹]	252.2	104.3	128.1
$X_E^{[e]}$ [%]	91	37	46

[a] M_n and polydispersity as was determined by high-temperature gel-permeation chromatography (HT GPC). [b] Molecular weight of the diblock copolymer as was calculated by ¹H NMR spectroscopy by using relative intensities of repeating unit signals and end-group signals and M_n of PE as was determined by HT GPC. [c] Weight fraction of PLA in the diblock copolymer calculated by using NMR spectroscopy and the densities at 25 °C reported for the respective components [PLA = 1.25,^[29] LPE = 0.95 (at 60% crystallinity)].^[30] [d] Taken as the peak of the melting endotherm (or the crystallization exotherm) during the heat (or cool) in DSC. [e] Percentage of crystallinity of the diblock copolymers calculated from $[\Delta H_m / (\Delta H_m^0)] \times 100\%$ with $\Delta H_m^0 = 277 \text{ J g}^{-1}$.^[31]

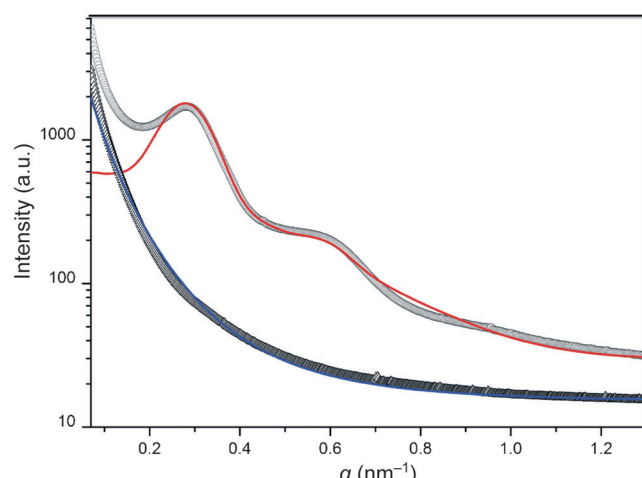


Figure 3. Radially averaged synchrotron SAXS patterns for PE-PLA(1) (○) and PE-PLA(2) (△) indicating a lamellar type and a disordered bicontinuous morphology, respectively. Color code: grey measured, red and blue simulated (PE-PLA(1) and PE-PLA(2) fits, respectively).

PLA(2) did not show pronounced peaks, which indicates a defined lattice. The fit shown in Figure 4 is based just on a simple-sphere-particle model.

The microphase-separated diblock copolymers were submerged in a NaOH/water/methanol mixture to remove the PLA block (Figure 2). The completion of the etching process was confirmed by FTIR spectroscopy. Removing the PLA block of microphase-separated PE-PLA(1) afforded a PE material that can be best described as PE nanofibers/ribbons as was indicated by SEM (Figure 4c and d). The PE layers may fold to fibers/ribbons during PLA removal in water. Microphase separation of PE-PLA(2) resulted in disordered bicontinuous morphology. The resultant morphology was mainly driven by both copolymer PE-PLA(2) and homopolymer PE present in the sample. Upon etching the

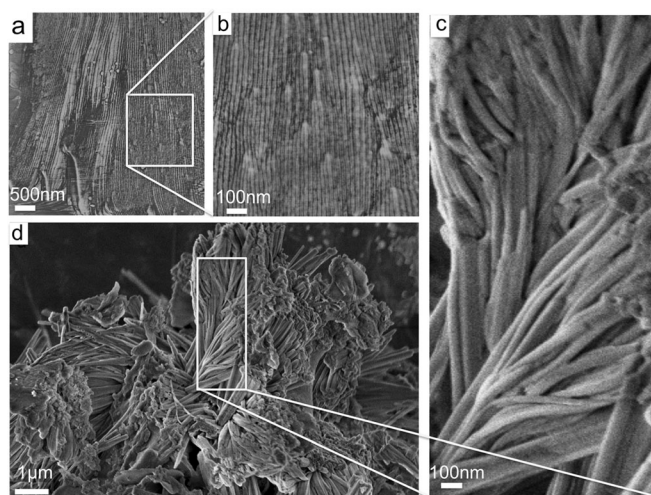


Figure 4. Microphase-separated PE-PLA(1). AFM phase images show a lamella-type morphology (a,b). SEM images of PE nanofibers/ribbons after etching (c,d).

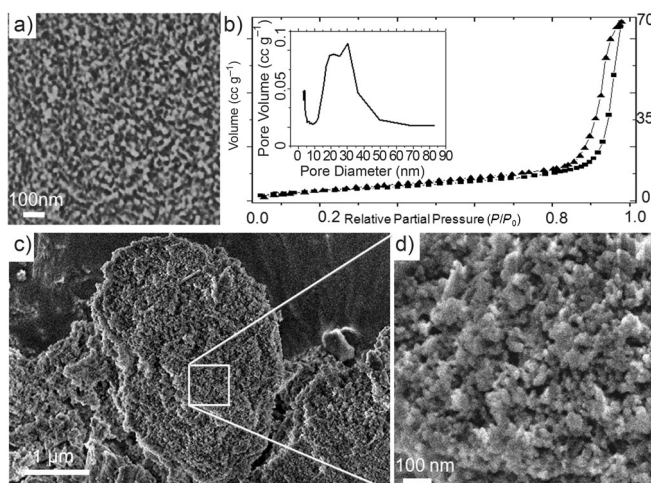


Figure 5. Microphase-separated PE-PLA(2). AFM image. Phase image shows the disordered bicontinuous morphology (a). Nitrogen adsorption (■)/desorption (▲) studies and inset of the resulting pore-size distribution (b). SEM images of porous PE after etching (c,d).

lactide block, the PE-PLA(2) gave rise to a porous PE material with a mean pore-size diameter of 30 nm as was determined by nitrogen adsorption/desorption studies (Barrett–Joyner–Helenda method, Figure 5b).

The pore size is in an acceptable agreement with the domain size of microphase-separated PE-PLA(2) as was observed by AFM (Figure 5a). A surface area of 19 m² g⁻¹ was calculated for the porous PE by using the Brunauer–Emmett–Teller (BET) method. The pores in the range of 10–50 nm contribute mainly to that specific surface. SEM studies (Figure 5c and d) supported the porous nature of the PE material and the structuring indicated by AFM studies (Figure 5a).

In summary, two main conclusions can be drawn from this study: 1) monoguanidinato titanium complexes are efficient

catalysts to give OH end-group-functionalized polyethylene (PE-OH) through a catalyzed version of Ziegler's "Aufbaureaktion"; and 2) Mesoporous polyethylene or polyethylene nanofibers/ribbons can be derived from PE-OH by diblock copolymer synthesis, microphase separation, and etching of the sacrificial polylactide block.

Acknowledgements

This work was supported by the DFG, SFB 840 and Sasol Germany GmbH. We thank Dr. Christine Denner for SEM investigations and Markus Hund for his support in the AFM lab.

Keywords: mesoporous materials • nanostructures • polyethylene • polymerization • titanium

- [1] R. Kempe, *Chem. Eur. J.* **2007**, *13*, 2764–2773.
- [2] L. R. Sita, *Angew. Chem.* **2009**, *121*, 2500–2508; *Angew. Chem. Int. Ed.* **2009**, *48*, 2464–2472.
- [3] a) E. G. Samsel, Ethyl Corporation, EP 0539876, **1992**; b) E. G. Samsel, D. C. Eisenberg, Ethyl Corporation, EP 0574854, **1993**.
- [4] a) J.-F. Pelletier, A. Mortreux, X. Olonde, K. Bujadoux, *Angew. Chem.* **1996**, *108*, 1980–1982; *Angew. Chem. Int. Ed. Engl.* **1996**, *35*, 1854–1856; b) J.-F. Pelletier, K. Bujadoux, X. Olonde, E. Adisson, A. Mortreux, T. Chenal, US 5779942, **1998**; c) T. Chenal, X. Olonde, J.-F. Pelletier, K. Bujadoux, A. Mortreux, *Polymer* **2007**, *48*, 1844–1856.
- [5] a) G. J. P. Britovsek, S. A. Cohen, V. C. Gibson, P. J. Maddox, M. van Meurs, *Angew. Chem.* **2002**, *114*, 507–509; *Angew. Chem. Int. Ed.* **2002**, *41*, 489–491; b) G. J. P. Britovsek, S. A. Cohen, V. C. Gibson, M. van Meurs, *J. Am. Chem. Soc.* **2004**, *126*, 10701–10712; c) M. van Meurs, G. J. P. Britovsek, V. C. Gibson, S. A. Cohen, *J. Am. Chem. Soc.* **2005**, *127*, 9913–9923; d) H. Kaneyoshi, Y. Inoue, K. Matyjaszewski, *Macromolecules* **2005**, *38*, 5425–5435; e) J. O. Ring, R. Thomann, R. Mühlaupt, J.-M. Raquez, P. Degee, P. Dubois, *Macromol. Chem. Phys.* **2007**, *208*, 896–902.
- [6] a) W. Zhang, L. R. Sita, *J. Am. Chem. Soc.* **2008**, *130*, 442–443; b) W. Zhang, J. Wei, L. R. Sita, *Macromolecules* **2008**, *41*, 7829–7833; c) J. Wei, W. Zhang, R. Wickham, L. R. Sita, *Angew. Chem.* **2010**, *122*, 9326–9330; *Angew. Chem. Int. Ed.* **2010**, *49*, 9140–9144; d) C. Giller, G. Gururajan, L. Wie, W. Zhang, W. Hwang, D. B. Chase, J. F. Rabolt, L. R. Sita, *Macromolecules* **2011**, *44*, 471–482.
- [7] a) D. J. Arriola, E. M. Carnahan, P. D. Hustad, R. L. Kuhlman, T. T. Wenzel, *Science* **2006**, *312*, 714–719; b) P. D. Hustad, R. L. Kuhlman, D. J. Arriola, E. M. Carnahan, T. T. Wenzel, *Macromolecules* **2007**, *40*, 7061–7064; c) P. D. Hustad, R. L. Kuhlman, E. M. Carnahan, T. T. Wenzel, D. J. Arriola, *Macromolecules* **2008**, *41*, 4081–4089; d) R. L. Kuhlman, T. T. Wenzel, *Macromolecules* **2008**, *41*, 4090–4094; e) A. Hotta, E. Cochran, J. Ruokolainen, V. Khanna, G. H. Fredrickson, E. J. Kramer, Y.-W. Shin, F. Shimizu, A. E. Cheriyan, P. D. Hustad, J. M. Rose, G. W. Coates, *Proc. Natl. Acad. Sci. USA* **2006**, *103*, 15327–15332; f) T. T. Wenzel, D. J. Arriola, E. M. Carnahan, P. D. Hustad, R. L. Kuhlman in *Topics in Organometallic Chemistry*, Vol. 26 (Ed.: Z. Guan), Springer, Berlin, Heidelberg, **2009**, pp. 65–104; g) S. Li, R. A. Register, B. G. Landes, P. D. Hustad, J. D. Weinhold, *Macromolecules* **2010**, *43*, 4761–4770; h) P. D. Hustad, G. R. Marchand, E. I. Garcia-Meinert, P. L. Roberts, J. D. Weinhold, *Macromolecules* **2009**, *42*, 3788–3794; i) F. Deplace, Z. Wang, N. A. Lynd, A. Hotta, J. M. Rose, P. D. Hustad, J. Tian, H. Ohtaki, G. W. Coates, F. Shimizu, K. Hirokane, F. Yamada, Y.-W. Shin, L. Rong, J. Zhu, S. Toki, B. S. Hsiao, G. H. Fredrickson, E. J. Kramer, *J. Polym. Sci. B: Polym. Phys.* **2010**, *48*, 1428–1437.
- [8] W. P. Kretschmer, A. Meetsma, B. Hessen, T. Schmalz, S. Qayyum, R. Kempe, *Chem. Eur. J.* **2006**, *12*, 8969–8978.
- [9] a) J. S. Rogers, G. C. Bazan, *Chem. Commun.* **2000**, 1209–1210; b) G. C. Bazan, J. S. Rogers, C. C. Fang, *Organometallics* **2001**, *20*, 2059–2064; c) C. J. Han, M. S. Lee, D.-J. Byun, S. Y. Kim, *Macromolecules* **2002**, *35*, 8923–8925; d) G. Mani, F. P. Gabbai, *Angew. Chem.* **2004**, *116*, 2313–2316; *Angew. Chem. Int. Ed.* **2004**, *43*, 2263–2266; e) G. Mani, F. P. Gabbai, *J. Organomet. Chem.* **2005**, *690*, 5145–5149; f) C. Döring, W. P. Kretschmer, R. Kempe, *Eur. J. Inorg. Chem.* **2010**, 2853–2860; g) W. P. Kretschmer, T. Bauer, B. Hessen, R. Kempe, *Dalton Trans.* **2010**, *39*, 6847–6852.
- [10] J. Wei, W. Zhang, L. R. Sita, *Angew. Chem.* **2010**, *122*, 1812–1816; *Angew. Chem. Int. Ed.* **2010**, *49*, 1768–1772.
- [11] a) M. Bochmann, S. J. J. Lancaster, *J. Organomet. Chem.* **1995**, 497, 55–59; b) M. Bochmann, S. J. Lancaster, *Angew. Chem.* **1994**, *106*, 1715–1718; *Angew. Chem. Int. Ed. Engl.* **1994**, *33*, 1634–1647.
- [12] R. A. Petros, J. R. Norton, *Organometallics* **2004**, *23*, 5105–5107.
- [13] J. M. Camara, R. A. Petros, J. R. Norton, *J. Am. Chem. Soc.* **2011**, *133*, 5263–5273.
- [14] a) I. Haas, W. P. Kretschmer, R. Kempe, *Organometallics* **2011**, *30*, 4854–4867; b) K. Michie, R. F. Jordan, *Organometallics* **2004**, *23*, 460–470; c) S. Murtuza, O. L. Casagrande Jr., R. F. Jordan, *Organometallics* **2002**, *21*, 1882–1890.
- [15] a) H. Uehara, T. Yoshida, M. Kakiage, T. Yamanobe, T. Komoto, K. Nomura, K. Nakajima, M. Matsuda, *Macromolecules* **2006**, *39*, 3971–3974; b) H. Uehara, M. Kakiage, D. Sakuma, T. Yamanobe, N. Takano, A. Barraud, E. Meurville, P. Ryser, *ACS Nano* **2009**, *3*, 924–932.
- [16] B. H. Jones, T. P. Lodge, *J. Am. Chem. Soc.* **2009**, *131*, 1676–1677.
- [17] L. M. Pitet, M. A. Amendt, M. A. Hillmyer, *J. Am. Chem. Soc.* **2010**, *132*, 8230–8231.
- [18] F. Cesano, E. Groppo, F. Bonino, A. Damin, C. Lamberti, S. Bordiga, A. Zecchina, *Adv. Mater.* **2006**, *18*, 3111–3114.
- [19] S. Shen, A. Henry, J. Tong, R. Zheng, G. Chen, *Nat. Nanotechnol.* **2010**, *5*, 251–255.
- [20] a) H. Kaneyoshi, K. Matyjaszewski, *J. Appl. Polym. Sci.* **2007**, *105*, 3–13; b) W. Wang, R. Liu, Z. Li, C. Meng, Q. Wu, F. Zhu, *Macromol. Chem. Phys.* **2010**, *211*, 1452–1459.
- [21] For a review please see: R. Kempe, *Z. Anorg. Allg. Chem.* **2010**, *636*, 2135–2147.
- [22] C. Döring, R. Kempe, *Eur. J. Inorg. Chem.* **2009**, 412–418.
- [23] A. Noor, W. P. Kretschmer, G. Glatz, R. Kempe, *Inorg. Chem.* **2011**, *50*, 4598–4606.
- [24] M. Hafeez, W. P. Kretschmer, R. Kempe, *Eur. J. Inorg. Chem.* **2011**, 5512–5522.
- [25] C. Jones, *Coord. Chem. Rev.* **2010**, *254*, 1273–1289.
- [26] E. Benzing, W. Kornicker, *Chem. Ber.* **1961**, *94*, 2263–2267.
- [27] G. J. P. Britovsek, V. C. Gibson, D. F. Wass, *Angew. Chem.* **1999**, *111*, 448–468; *Angew. Chem. Int. Ed.* **1999**, *38*, 428–447.
- [28] Y. Wang, M. A. Hillmyer, *J. Polym. Sci. Part A* **2001**, *39*, 2755–2766.
- [29] D. R. Witzke, J. J. Kolstad, R. Narayan, *Macromolecules* **1997**, *30*, 7075–7085.
- [30] A. J. Peacock, *Handbook of Polyethylene*, Marcel Dekker, Basel, **2000**.
- [31] R. Wu, T. F. Al-Azemi, K. S. Bisht, *Chem. Commun.* **2009**, 1822–11824.
- [32] S. Förster, L. Apostol, W. Bras, *J. Appl. Crystallogr.* **2010**, *43*, 639–646.
- [33] a) S. C. Schmidt, M. A. Hillmyer, *J. Polym. Sci. B: Polym. Phys.* **2002**, *40*, 2364–2376; b) M. W. Matsen, *Eur. Phys. J. E* **2007**, *21*, 199–207; c) N. A. Lynd, M. A. Hillmyer, *Macromolecules* **2005**, *38*, 8803–8810.

Received: July 13, 2012

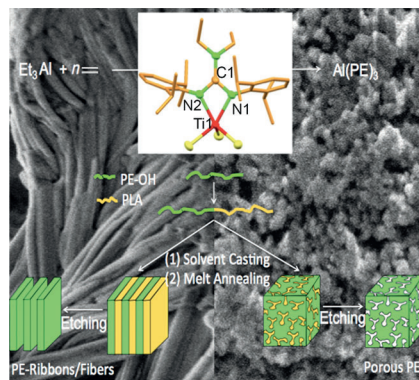
Revised: August 17, 2012

Published online: ■■■, 0000

Nanostructures

S. K. T. Pillai, W. P. Kretschmer,
M. Trebbin, S. Förster,
R. Kempe* ■■■—■■■

Tailored Nanostructuring of End-Group-Functionalized High-Density Polyethylene Synthesized by an Efficient Catalytic Version of Ziegler's "Aufbaureaktion"



Monoguanidinato titanium complexes are efficient catalysts to make OH end-group-functionalized polyethylene (PE-OH) by a catalyzed version of Ziegler's "Aufbaureaktion". This PE-OH can be structured to mesoporous polyethylene or polyethylene nanofibers/ribbons through diblock copolymer synthesis, microphase separation, and etching of the sacrificial polylactide block.